

Characterization of the dynamic properties of *Rhodobacter capsulatus* ferricytochrome c' – a 28 kDa paramagnetic heme protein

Michael Caffrey^a, Jean-Pierre Simorre^a, Michael Cusanovich^b, Dominique Marion^{a,*}

^aInstitut de Biologie Structurale Jean-Pierre Ebel (CNRS-CEA), 41 avenue des Martyrs, 38027 Grenoble Cédex, France

^bDepartment of Biochemistry, University of Arizona, Tucson, AZ 85721, USA

Received 23 March 1995; revised version received 5 June 1995

Abstract The cytochromes c' are paramagnetic heme proteins generally consisting of two identical 14 kDa subunits. The recent assignment of the ¹H and ¹⁵N resonances of the *Rhodobacter capsulatus* ferricytochrome c' has allowed characterization of the dynamic properties by measurement of the heteronuclear NOE for each resolved amide group. The relative importance of fast local motion and paramagnetic effect on nuclear relaxation were distinguished by comparison of the measured heteronuclear NOE with that of the overall experimental average. We show that the average experimental value of −0.16 corresponds to the rigid body motion expected for a spherical complex of 28 kDa. Residues 3–5, 50–55 and 69–70 exhibit decreased heteronuclear NOE due to local motions on a fast time scale with respect to molecular tumbling. Based on the X-ray crystal structure of the homologous cytochrome c' from *Chromatium vinosum*, the mobile regions correspond to the N-terminus of helix-1 and 2 regions of nonregular secondary structure located between helices-2 and -3.

Key words: Four helix bundle; Heteronuclear; NMR; NOE; Relaxation

1. Introduction

The cytochromes c' are paramagnetic heme proteins, which generally consist of two identical 14 kDa subunits. They are widely found in photosynthetic prokaryotes and their concentration levels increase under photosynthetic growth conditions [1]. Although their exact function in vivo is at present unknown, they presumably are involved in a metabolic pathway active during photosynthesis. Interestingly, the cytochromes c' from some species of bacteria bind CO in a cooperative manner [2], while cytochromes c' from other species of bacteria bind CO non-cooperatively [3]. As a consequence of their ligand binding properties, the cytochromes c' serve as simple dimeric models of cooperative interactions in proteins. Each subunit of the cytochromes c' possesses a four-helix bundle structural motif as derived from X-ray crystal structures of the cytochromes c' from *Rsp. molischianum* [4], *Rsp. rubrum* [5] and *C. vinosum* [6]. Recently, we have extensively assigned the ¹H, ¹³C and ¹⁵N resonances of the ferricytochrome c' from *Rb. capsulatus* [7]. The NMR data show that the *Rb. capsulatus* cytochrome c' possesses a four-helix bundle structural motif, which is most homologous to the cytochromes c' of *Rsp. rubrum* and *C. vino-*

sum. Together, the X-ray and NMR studies provide a significant amount of structural data for the cytochromes c'. In contrast, very little is known about the dynamic properties of the cytochromes c'. In what follows, we characterize the global and local motions of *Rb. capsulatus* ferricytochrome c' by determination of the heteronuclear NOE for backbone amide groups.

2. Materials and methods

The protein preparation and resonance assignments have been described elsewhere [7]. All NMR experiments were performed on a Bruker AMX-600 spectrometer equipped with a broadband probe. Experimental conditions were 8 mM ferricytochrome c' (heme concentration) in 100 mM PO₄ (pH = 6.0), 25 μM chloramphenicol and 10% D₂O at 300 K. The pulse sequences used for determination of the heteronuclear NOE were similar to those proposed by Peng and Wagner [8]. Modifications of the published pulse sequences included: (1) WALTZ-16 composite decoupling [9] for ¹H saturation (field strength = 12 kHz) instead of a train of 180° ¹H pulses; (2) addition of the WATERGATE sequence [10] for water suppression. Spectral widths for ¹H and ¹⁵N were 6.4 and 30 ppm, respectively. Carrier positions for ¹H and ¹⁵N were 8.40 and 117.4 ppm, respectively. Spectra were acquired with 100 complex points in *t*₁ and 512 complex points in *t*₂. For each experiment, 64 scans per *t*₁ increment were recorded with a relaxation delay of 3 s between scans, resulting in an overall experimental time of 6 h. The field strength for WALTZ-16 decoupling of ¹⁵N was 2.1 kHz. Quadrature detection in the *t*₁ dimension was obtained by the TPPI-States method [11]. All data were processed and analyzed using the program FELIX version 2.1 (Biosym Technologies). The indirect dimensions of the data sets were multiplied by a skewed sine bell function and zero-filled to result in 512 × 256 matrices. For calculation of the heteronuclear NOE, the maximum intensity of ¹H–¹⁵N correlations were determined using the peak-pick subroutine of FELIX. The S.E. of the heteronuclear NOE was estimated as in [12].

3. Results and discussion

Before discussing the results of the relaxation experiments, it is of interest to discuss the theory of the heteronuclear NOE. The heteronuclear NOE is given by:

$$\text{NOE} = \frac{I_{\text{sat}} - I_{\text{eq}}}{I_{\text{eq}}} = \frac{\gamma_{\text{H}} \times R_{\text{Hz} \rightarrow \text{Nz}}}{\gamma_{\text{N}} \times R_{\text{Nz}}}, \quad (1)$$

where *I*_{sat} is the cross peak intensity when ¹H are saturated, *I*_{eq} is the equilibrium Zeeman intensity, γ_H is the gyromagnetic ratio for ¹H, γ_N is the gyromagnetic ratio for ¹⁵N, *R*_{Nz} is the ¹⁵N longitudinal relaxation rate, and *R*_{H_z→N_z} is the cross relaxation rate [13]. In paramagnetic macromolecules, ¹⁵N longitudinal relaxation rate is described by:

$$R_{\text{Nz}}^{\text{obs}} = R_{\text{Nz}}^{\text{dm}} + R_{\text{Nz}}^{\text{pm}}, \quad (2)$$

where *R*_{Nz}^{obs}, *R*_{Nz}^{dm} and *R*_{Nz}^{pm} are the observed, diamagnetic and

*Corresponding author. Fax: (33) (76) 885 494.

Abbreviations: HSQC, heteronuclear single quantum coherence spectroscopy; NMR, nuclear magnetic resonance; NOE, nuclear Overhauser effect; TPPI, time proportional phase incrementation.

paramagnetic ^{15}N longitudinal relaxation rates, respectively. The diamagnetic terms are made up of dipolar and chemical anisotropy components. In the case of the heteronuclear NOE, the terms of interest are defined as:

$$R_{\text{Hz} \rightarrow \text{Nz}} = \left[\frac{\gamma_{\text{H}}^2 \gamma_{\text{N}}^2 \hbar^2}{4r_{\text{HN}}^6} \right] [6J(\omega_{\text{H}} + \omega_{\text{N}}) - J(\omega_{\text{H}} - \omega_{\text{N}})], \quad (3)$$

$$R_{\text{Nz}}^{\text{dm}} = \left[\frac{\gamma_{\text{H}}^2 \gamma_{\text{N}}^2 \hbar^2}{4r_{\text{HN}}^6} \right] [J(\omega_{\text{H}} - \omega_{\text{N}}) + 3J(\omega_{\text{N}}) + 6J(\omega_{\text{H}} + \omega_{\text{N}})] + \frac{\Delta\sigma^2 \omega_{\text{N}}^2}{3} [J(\omega_{\text{N}})], \quad (4)$$

where \hbar is Planck's constant divided by 2π , r_{HN} is the length of the H–N bond vector, $J(\omega)$ is the spectral density as a function of Larmor frequencies for $^1\text{H}(\omega_{\text{H}})$ and $^{15}\text{N}(\omega_{\text{N}})$, and $\Delta\sigma$ is the chemical shift anisotropy value [8]. The paramagnetic term is made up of dipolar, contact and Curie terms [14]. For the present case, the ^1H and ^{15}N nuclei of backbone amide groups are not in contact with the heme iron and thus the contact term is not operative. Furthermore, at high magnetic fields Curie relaxation is negligible to longitudinal relaxation [14]. Accordingly, $R_{\text{Nz}}^{\text{pm}}$ is defined by:

$$R_{\text{Nz}}^{\text{pm}} = \left[\frac{2S(S+1) \gamma_{\text{s}}^2 \gamma_{\text{N}}^2 \hbar^2}{15r_{\text{NS}}^6} \right] \times [J(\omega_{\text{N}} - \omega_{\text{s}}) + 3J(\omega_{\text{N}}) + 6J(\omega_{\text{N}} + \omega_{\text{s}})], \quad (5)$$

where S is the total electron spin, γ_{s} is the gyromagnetic ratio for the electron, and r_{NS} is the electron–nuclear distance. Since $\omega_{\text{s}} \gg \omega_{\text{N}}$, equation (5) simplifies to:

$$R_{\text{Nz}}^{\text{pm}} = \left[\frac{2S(S+1) \gamma_{\text{s}}^2 \gamma_{\text{N}}^2 \hbar^2}{15r_{\text{NS}}^6} \right] [3J(\omega_{\text{N}}) + 7J(\omega_{\text{s}})], \quad (6)$$

As a consequence of the $1/r_{\text{NS}}^6$ term in equation (6), the paramagnetic effect on the heteronuclear NOE is highly dependent upon the nuclear–electron distance ranging from being the dominant term in relaxation (i.e. $R_{\text{Nz}}^{\text{pm}} \gg R_{\text{Nz}}^{\text{dm}}$) for nuclei proximal to the free electron (i.e. Fe^{3+} center) to a negligible term (i.e. $R_{\text{Nz}}^{\text{pm}} \ll R_{\text{Nz}}^{\text{dm}}$) for nuclei distant from the iron. In Fig. 1, the relative magnitude of the paramagnetic effect on heteronuclear ^1H – ^{15}N NOE is plotted as a function of the effective correlation time for nuclei at different distances from a paramagnetic center possessing 5 unpaired electrons as is the case for ferricytochrome c' . First note that in the absence of a paramagnetic effect (i.e. nuclei that are $>15 \text{ \AA}$ from the paramagnetic center), the heteronuclear NOE exhibits the well-known dependence on correlation time, ranging from a minimum of approximately -5 at correlation times less than 0.1 ns to a maximum of approximately -0.15 at correlation times greater than 10 ns . In the case of paramagnetic proteins, the presence of free electrons tends to 'dilute' the heteronuclear NOE due to an increase in $R_{\text{Nz}}^{\text{pm}}$. Thus, amide groups that exhibit decreased NOE (i.e. more negative) with respect to the average are undergoing fast local motions, characteristic of residues at the protein termini or in

unstructured loops. In contrast, amide groups that exhibit increased NOE (i.e. more positive) with respect to the average are within 15 \AA of the paramagnetic center. Importantly, the relative magnitudes of the dynamic and paramagnetic effects vary with correlation time. For example, dynamic effects are most pronounced in larger molecules exhibiting relatively long correlation times; paramagnetic effects are most pronounced for smaller molecules exhibiting relatively short correlation times.

In Fig. 2, the heteronuclear ^1H – ^{15}N NOE of *Rb. capsulatus* ferricytochrome c' are plotted as a function of residue number. The experimentally determined average corresponds to -0.16 . The correlation time for a 28 kDa spherical complex is estimated to be 11 ns using the Stokes–Einstein equation [15]. From equations (1), (3) and (4), the heteronuclear NOE of the cytochrome c' is estimated to be -0.15 . Consequently, the average heteronuclear NOE is consistent with that of a dimer, in agreement with previous observations by sedimentation equilibrium which suggested an apparent molecular weight of 23 kDa [16].

Equation (6) shows that the Fe–N distance could possibly be quantitated and subsequently used as supplementary information for the calculation of a structure by NMR. Indeed, several residues, such as 12, 18, 19, 115 and 117, appear to exhibit heteronuclear NOE that are significantly increased with respect to the average. Interestingly, in the crystal structure of the homologous cytochrome c' from *C. vinosum*, the ^{15}N of the equivalent residues are less than 15 \AA from the Fe center. However, it is important to note that heteronuclear NOE that are larger than the theoretical maximum can also be caused by factors other than paramagnetism. First, the heteronuclear NOE of large molecules are difficult to quantitate because one is determining a small difference between 2 relatively large numbers. Second, magnetization transfer between saturated water and exchangeable NH or incomplete proton saturation lead to overestimates of the heteronuclear NOE. However, the present experiments were performed without water presaturation. Furthermore, the correspondence between the average heteronuclear NOE and that expected for rigid body motion

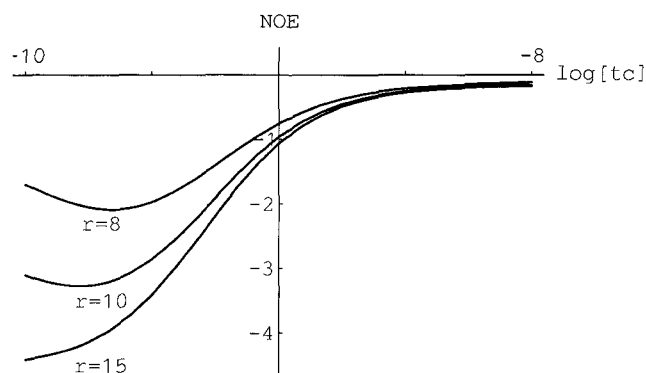


Fig. 1. Simulation of heteronuclear ^1H – ^{15}N NOE as a function of correlation time for ^{15}N at different distances (given in units of \AA) from a paramagnetic center. In this simulation, the heteronuclear NOE has been calculated using equations (1), (3), (4) and (6) given in the text. The spectral density function in equations (3) and (4) were defined as $J(\omega) = 0.4\tau_{\text{c}}/(1 + \omega^2\tau_{\text{c}}^2)$ where τ_{c} is the correlation time. The spectral density function in equation (6) was defined as $J(\omega) = 0.4\tau_{\text{s}}/(1 + \omega^2\tau_{\text{s}}^2)$ where τ_{s} is the correlation time of the electron. The constants were: $\tau_{\text{s}} = 0.05 \text{ ns}$ [14], $S = 5/2$, $\gamma_{\text{N}} = 2.71 \times 10^3 \text{ rads} \cdot \text{s}^{-1} \cdot \text{G}^{-1}$, $\gamma_{\text{s}} = 1.76 \times 10^7 \text{ rads} \cdot \text{s}^{-1} \cdot \text{G}^{-1}$, $\hbar = 1.05 \times 10^{-27} \text{ erg} \cdot \text{s} \cdot \text{rad}^{-1}$, $\omega_{\text{s}} = 395 \text{ GHz}$, $\omega_{\text{N}} = 60.81 \text{ MHz}$, $\omega_{\text{H}} = 600.13 \text{ MHz}$, $r_{\text{HN}} = 1.02 \text{ \AA}$ [18], and $\Delta\sigma = -160 \text{ ppm}$ [19].

(Fig. 2) suggests that complete saturation of the protons was achieved in the experiment. Therefore, we feel that paramagnetic relaxation is the most likely cause of the anomalous heteronuclear NOE. Nonetheless, in the case of relatively large paramagnetic proteins such as the cytochromes *c'*, characterization of other relaxation parameters are more appropriate for extracting structural information. For example, the transverse relaxation rates increase with decreasing distance to the paramagnetic center and can be determined more accurately than the heteronuclear NOE [17].

As shown in Fig. 2, residues 3–5, 50–55 and 69–70 exhibit decreased heteronuclear NOE with respect to the average value. The only explanation for the decreased NOE (i.e. more negative) of these residues is that these regions of the backbone are undergoing local motions on a fast time scale with respect to molecular tumbling. Note that the present data do not exclude mobility in other regions of the protein, which might be spatially near the Fe center and hence exhibit NOE that are diluted by paramagnetic relaxation. From Fig. 1, the effective correlation time of the fast local motions is estimated to be between 1 and 10 ns. It is of interest to consider the location of the mobile regions in the 3D structure. At present, there is no high resolution structure available for the *Rb. capsulatus* cytochrome *c'*. Accordingly, we have chosen to consider the X-ray crystal structure of the cytochrome *c'* from *C. vinosum* [6], which has been previously shown by NMR to be structurally homologous to the *Rb. capsulatus* ferricytochrome *c'* [7]. In Fig. 3A, the ribbon representation is shown for one of the monomeric subunits of the *C. vinosum* ferricytochrome *c'*. In this figure, regions exhibiting fast local motions are depicted in black and the regions that are presumably in rigid body motion are depicted in gray. The first mobile region comprising residues 3–5 occurs at the N-terminus of helix-1. The second mobile region comprising residues 50–55 occurs in a region of non-regular secondary structure which follows helix-2. Previously, the $^3J_{\text{HN}\alpha}$ coupling constants and short-range NOE of this region in *Rb. capsulatus* cytochrome *c'* were shown to be consistent with a region of non-regular secondary structure [7], which is similar to that observed in the crystal structure of *C. vinosum* cytochrome *c'* [6]. In contrast, the equivalent resi-

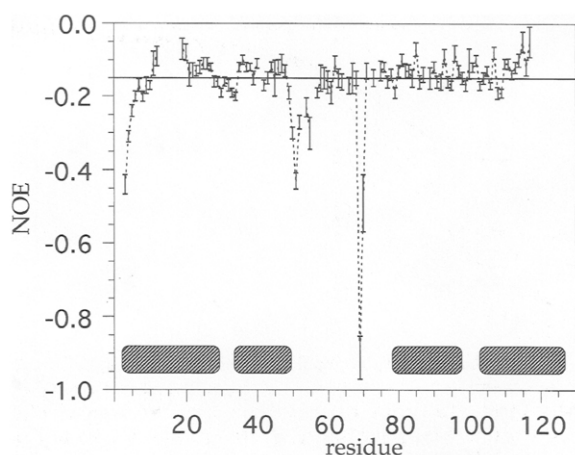


Fig. 2. Observed heteronuclear NOE as a function of residue number. The solid horizontal line corresponds to the theoretical NOE for rigid body motion. Breaks in the lines connecting the data correspond to proline residues, which lack an amide group, or to unassigned amide groups. Helical regions, deduced by NMR [7], are presented as hatched cylinders.

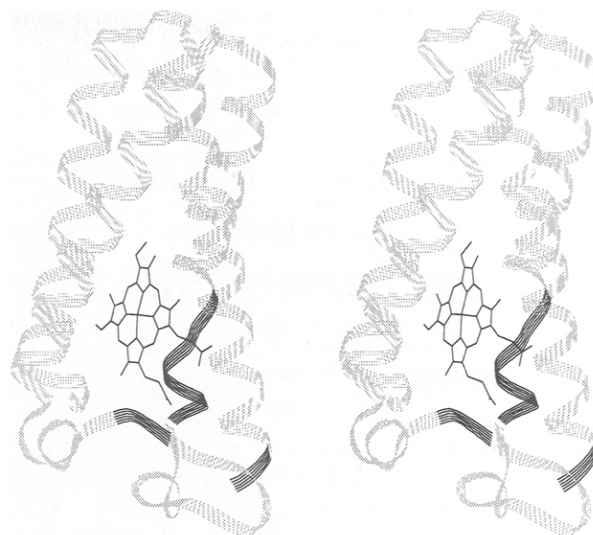


Fig. 3. Model of *Rb. capsulatus* ferricytochrome *c'* structure based on the x-ray structure of *C. vinosum* ferricytochrome *c'* [6] and the amino acid sequence alignment of [1]. Mobile regions are depicted in black.

dues of *Rps. molischianum* cytochrome *c'* are in a helix conformation [4]. The third mobile region comprising of residues 69–70 occurs in a region of non-regular secondary structure. Interestingly, the three mobile regions are located in close spatial proximity to the heme, which presumably plays an important functional role. Furthermore, the mobile regions are in close spatial proximity to one another, suggesting that their motional properties might be concerted. In contrast, the mobile regions of one subunit are relatively distant from the residues of the other subunit (not shown).

In conclusion, we have shown that the average heteronuclear NOE can be used to distinguish between fast local motion and paramagnetic effects on nuclear relaxation rates in paramagnetic proteins. In *Rb. capsulatus* ferricytochrome *c'*, the mobile regions appear in three regions that are in close spatial contact. To our knowledge, the present work represents the first NMR characterization of the dynamic properties of a cytochrome *c'*. Further, the present work lends insight into the dynamic properties of a multisubunit protein. It is anticipated that further characterization of the structural and dynamic properties of the cytochromes *c'* will be instrumental for their use as models of cooperative interactions in proteins.

Acknowledgements: This work was supported in part by the Commissariat à l'Energie Atomique (CEA), the Centre National de la Recherche Scientifique (CNRS), Biosym Technologies, and the United States Public Health Services (Grant GM 21277 to M. Cusanovich). This is Publication 271 of the Institut de Biologie Structurale Jean-Pierre Ebel.

References

- [1] Meyer, T. and Kamen, M. (1982) *Advanc. Protein Chem.* 35, 105–212.
- [2] Doyle, M., Gill, S. and Cusanovich, M. (1986) *Biochemistry* 25, 2509–2516.
- [3] Doyle, M., Weber, P. and Gill, S. (1985) *Biochemistry* 24, 1987–1991.
- [4] Finzel, B., Weber, P., Hardman, K. and Salemme, F. (1985) *J. Mol. Biol.* 186, 627–643.

- [5] Yasui, M., Harada, S., Kai, Y., Kasai, N., Kusunoki, M. and Matsuura, N. (1992) *J. Biochem. (Tokyo)* 111, 317–324.
- [6] Ren, Z., Meyer, T. and McRee, D. (1993) *J. Mol. Biol.* 234, 433–445.
- [7] Caffrey, M., Simorre, J.-P., Brutscher, B., Cusanovich, M. and Marion, D. (1995) *Biochemistry* 34, 5904–5912.
- [8] Peng, J. and Wagner, G. (1992) *J. Magn. Reson.* 98, 308–332.
- [9] Shaka, A., Keeler, J., Frenkiel, T. and Freeman, R. (1983) *J. Magn. Reson.* 52, 335–338.
- [10] Sklenář, V., Piotto, M., Leppik, R. and Saudek, V. (1993) *J. Magn. Reson.* 102, 241–245.
- [11] Marion, D., Ikura, M., Tschudin, R. and Bax, A. (1989) *J. Magn. Reson.* 85, 393–399.
- [12] Farrow, N., Muhandiram, R., Singer, A., Pascal, S., Kay, C., Gish, G., Shoelson, S., Pawson, T., Forman-Kay, J. and Kay, L. (1994) *Biochemistry* 33, 5984–6003.
- [13] Nogge, J. and Schirmer, R. (1971) in *The Nuclear Overhauser Effect*, Academic Press, New York.
- [14] Banci, L., Luchinat, C. and Bertini, L. (1991) in *Nuclear and Electron Relaxation*, VCH Publishers, Inc., Weinheim.
- [15] Cantor, C. and Schimmel, P. (1980) in *Biophysical Chemistry*, W.H. Freeman & Company, San Francisco.
- [16] Cusanovich, M. (1971) *Biochem. Biophys. Acta* 236, 238–241.
- [17] Torchia, D., Nicholson, L., Cole, H. and Kay, L. (1993) in *NMR of Proteins* (Clare, G. and Gronenborn, A., Eds.) pp. 190–219, MacMillan Press, Ltd., London.
- [18] Kieter, E. (1986) Ph.D. Thesis, University of Illinois.
- [19] Hiyama, Y., Niu, C., Silverton, J., Bravaso, A. and Torchia, D. (1988) *J. Am. Chem. Soc.* 110, 2378–2383.